Am J Physiol Endocrinol Metab 319: E354–E362, 2020.
First published June 30, 2020; doi:10.1152/ajpendo.00114.2020.

RESEARCH ARTICLE

Spinophilin-deficient mice are protected from diet-induced obesity and insulin resistance

Yong Zhang,[1,2] Lili Song,[1] Huansheng Dong,[1,2] Do-sung Kim,[1] Zhen Sun,[1] Heather Boger,[3] Qin Wang,[4] and Hongjun Wang[1,5]

[1]*Department of Surgery, Medical University of South Carolina, Charleston, South Carolina;* [2]*College of Life Sciences, Qingdao Agricultural University, Qingdao, People's Republic of China;* [3]*Department of Neuroscience, Medical University of South Carolina, Charleston, South Carolina;* [4]*Department of Cell, Developmental and Integrative Biology, University of Alabama at Birmingham; and* [5]*Ralph H. Johnson Veterans Affairs Medical Center, Charleston, South Carolina*

Submitted 25 March 2020; accepted in final form 16 June 2020

Zhang Y, Song L, Dong H, Kim DS, Sun Z, Boger H, Wang Q, Wang H. Spinophilin-deficient mice are protected from diet-induced obesity and insulin resistance. *Am J Physiol Endocrinol Metab* 319: E354–E362, 2020. First published June 30, 2020; doi:10.1152/ajpendo.00114.2020.—Browning of white adipose tissue (WAT) has been shown to reduce obesity and obesity-related complications, suggesting that factors that promote WAT browning may have applications in the development of therapeutic strategies for treating obesity. Here, we show that ablation of spinophilin (SPL), a ubiquitously expressed, multidomain scaffolding protein, increases metabolism and improves energy balance. Male and female SPL knockout (KO) and wild-type (WT) littermate controls were fed a chow diet or a high-fat diet (HFD). Body weight, hepatic steatosis, glucose and insulin tolerance, physical activity, and expression of browning genes in adipose tissues were measured and compared. Male SPL knockout (KO) mice fed a chow diet were significantly leaner, had lower body weights, and exhibited better glucose tolerance and insulin sensitivity than wild-type (WT) littermate controls. When fed an HFD, SPL KO mice were protected from increased body fat, weight gain, hepatic steatosis, hyperinsulinemia, and insulin resistance. Physical activity of SPL KO mice was markedly increased compared with WT controls. Furthermore, expression of the brown adipocyte marker, uncoupling protein-1 (UCP-1), and the mitochondrial activity markers, cd137 and c-idea, were significantly increased in visceral WAT (vWAT) of SPL KO mice, suggesting that SPL knockout protected the mice from HFD-induced obesity and its metabolic complications, at least in part, by promoting the browning of white adipocytes in vWAT. Our data identify a critical role of SPL in regulating glucose homeostasis, obesity, and adipocyte browning. These results suggest SPL may serve as a drug target for obesity and diabetes.

activity; browning; insulin sensitivity; obesity; spinophilin

INTRODUCTION

Obesity and type 2 diabetes (T2D) have reached epidemic proportions globally because of sedentary life styles and excessive energy intake (20, 27). Obesity represents the most important risk factor for insulin resistance, T2D, hepatosteatosis, and cardiovascular diseases (14, 23, 27, 34). Factors that regulate high-fat diet-induced obesity may serve as therapeutic targets to reduce diet-related obesity and its associated disorders.

Correspondence: H. Wang (wangho@musc.edu).

Adipose tissue is generally divided into white adipose tissue (WAT) and brown adipose tissue (BAT). White adipocytes usually contain a single large lipid droplet and function as an energy storage and endocrine organ that secrete hormones that regulate feeding and satiety (30). Brown adipocytes are thermogenic cells packed with mitochondria and uniquely express uncoupling protein-1 (UCP-1) (28). BAT dissipates energy as heat in response to a cold environment, counteracts obesity, and protects against the detrimental effects of surplus energy intake (26). Expansion and/or activation of brown adipose tissue in animals counteracts diet-induced weight gain and ameliorates related disorders, such as T2D mellitus. Presence of BAT in adult humans is associated with a metabolic benefit, including lower body mass index and lower total adipose tissue content (13, 24). Recent studies have shown that a subset of white adipocytes can develop brown characteristics (a process called "browning"), and can become so-called "brite", or "beige" cells. Beige cells are interspersed in WAT and have distinct developmental origins and distinct molecular characteristics compared with white or brown adipocytes (29). Beige cells share similar properties with BAT, including UCP-1 expression and multifocal morphology, and their formation can be induced by cold, exercise, and other conditions (7, 18). The occurrence of beige cells and the conversion of white adipocytes into beige and brown adipocytes suggest plasticity between adipose tissue phenotypes (10). This offers the attractive therapeutic potential of promoting browning as a treatment strategy for obesity and its related complications. Since browning was first described (10), an ever-increasing list of agents, including specific gene modulation, food components, drugs, and environments, have been reported to promote browning and to counteract obesity (4, 41).

Spinophilin (SPL) is a ubiquitously expressed multidomain scaffolding protein that interacts with protein phosphatase 1 and F-actin (1, 33). More than 30 SPL-binding partners have been discovered. These include cytoskeletal and cell adhesion molecules, enzymes, guanine nucleotide exchange factors, regulators of G-protein signaling, membrane receptors, ion channels, and the tumor suppressor alternative reading frame (32). The physiological relevance of the interactions between SPL and some of these binding partners remains largely unknown. SPL modulates the activity of different G protein-coupled receptors (2, 8, 22, 40) and plays important functions in the nervous

system and in information transfer in immunological synapses (3, 15). SPL also appears to be a growth suppressor, and loss of SPL is associated with poor prognosis in cancer (16).

SPL expression is inversely related to heart rate in mice in a manner reflecting their metabolic activity and has been suggested to play a role in whole body metabolism and energy balance (11). Furthermore, SPL has been shown to regulate M3 muscarinic receptor-mediated insulin release in pancreatic β-cells, and SPL knockout mice showed reduced body weights associated with decreases in percentages of body fat mass compared with wild-type mice (31). Nevertheless, the mechanisms by which SPL regulates energy homeostasis, obesity, and insulin resistance remain largely elusive.

In this study, we found that ablation of SPL protects mice from a high-fat diet (HFD)-induced obesity and liver steatosis, improves whole body glucose homeostasis, and restores insulin sensitivity. Our data indicate that SPL ablation exerts these effects, at least in part, via promoting physical activity and browning in visceral white adipose tissue (vWAT). Thus, the data suggest that SPL plays a critical role in promoting energy expenditure and white to brown fat transition.

MATERIALS AND METHODS

Animals. SPL KO mice were originally described by Feng et al. (15), and they have been backcrossed for over 12 generations onto the C57BL/6 background (9). SPL KO mice and their wild-type (WT) littermates were generated by crossing heterozygous SPL mice. Mice genotyping was performed by PCR analysis using mouse tail DNA. Primer sequences for detection of SPL allele (493 bp): 5′-AGGATCTCCTGTCATCTCACCTTGCTCCTG-3′ (forward); 5′-AAGAACTCGTCAAGAAGGCGATAGAAGGCG-3′ (reverse); Primer sequences for wild-type SPL allele (558 bp): 5′-CACGTCCAGCTTGGATGGTCTTTT-3′ (forward) and 5′-CACTGCTCTGGCTTTCACGCTAGT-3′ (reverse). The PCR condition was 95°C for 3 min, then 35 cycles of 95°C for 40 s, 60°C for 40 s, 72°C for 1 min, and followed by 72°C for 7 min. Mice were maintained under a standard 12:12-h light-dark cycle. Food and water were available ad libitum. All animal experiments were approved by the Animal Care Committee at the Medical University of South Carolina. Both male and female mice were studied.

To examine the effect of spinophilin on diet-induced obesity, male and female Spl−/− and WT littermate mice ($n = 9$ in male and $n = 6$ in female groups) were fed either a control (chow) or HFD diet. Chow diet (D12450J; Research Diets, New Brunswick, NJ) contains 20% protein, 10% of fat, 70% of carbohydrate and energy density of 3.82 kcal/g. HFD (D12492, Research Diets) contains 20% of protein, 60% of fat, 20% of carbohydrate, and energy density of 5.21 kcal/g. The ratios of saturated/monounsaturated fat were 1:1.14 and 1:1.1, and the ratios of saturated/polyunsaturated fat were 1:2 and 1:1 for chow and HFD, respectively. Feeding was for 8 wk beginning from the age of 8 or 9 wk. Activities, including behavior, food intake, drinking, and licking were observed on a daily basis by two individual investigators, as previously described (12). Signs of illness, including ruffled fur, hunched posture, lethargy, and dehydration were also noted. Body weights were recorded every 3 days. Food intake (including possible spillage) was measured during a 24-h period every week. To measure rectal body temperature, mice were hand-restrained and placed on a horizontal surface. A temperature probe covered with Vaseline was gently inserted into the rectum with a depth of ~1 cm. The probe was carefully removed after obtaining the reading.

Intraperitoneal glucose tolerance tests and insulin tolerance tests. For the intraperitoneal glucose tolerance test (IPGTT), mice were fasted overnight and then injected with D-glucose (2 mg/g body wt ip). For the insulin tolerance test (ITT), mice were fasted for 5–6 h and then given an injection of human insulin (0.75 U/kg ip; Humulin, Eli Lily, Indianapolis, IN). A drop of blood was taken from the tail vein before (defined as *time 0* min) and 15, 30, 60, 90, and 120 min after glucose or insulin administration. Mice were immobilized in a mouse restrainer (Braintree Scientific) before blood collection to reduce stress. Blood glucose levels at each time point were measured using an Accu-Chek glucometer (LifeScan, Mountain View, CA). Area under the curve was calculated using the trapezoidal method. There was at least a 3-day interval between IPGTT and ITT measurements in the same group of mice.

Glucose-stimulated insulin secretion. Mice were fasted overnight and then injected intraperitoneally with D-glucose (3 mg/g body wt). Blood was collected from the tail vein at 0, 2, 5, 15, and 30 min postinjection. Insulin concentration in serum (5 μL) was analyzed using the Mouse Chemiluminescent Insulin ELISA kit according to the manufacturer's recommendations (cat. no. 80-INSMS-E01, sensitivity of 0.06 ng/mL; intra-assay and interassay coefficient of variation (CV): 7.4–11.4% and 8.3–13.2%; ALPCO, Salem, NH).

Tissue harvest, serum preparation, and blood biochemistry. Four weeks after all the tests, mice were given anesthesia, and blood was collected by retro-orbital bleeding into a heparinized tube. Plasma was separated by centrifugation and stored at −80°C for further analysis. Mice were then euthanized, and livers and fat tissues were collected, weighed, and snap frozen in liquid nitrogen for further analysis by RT-PCR, Western blot, and immunohistochemical analyses. Leptin

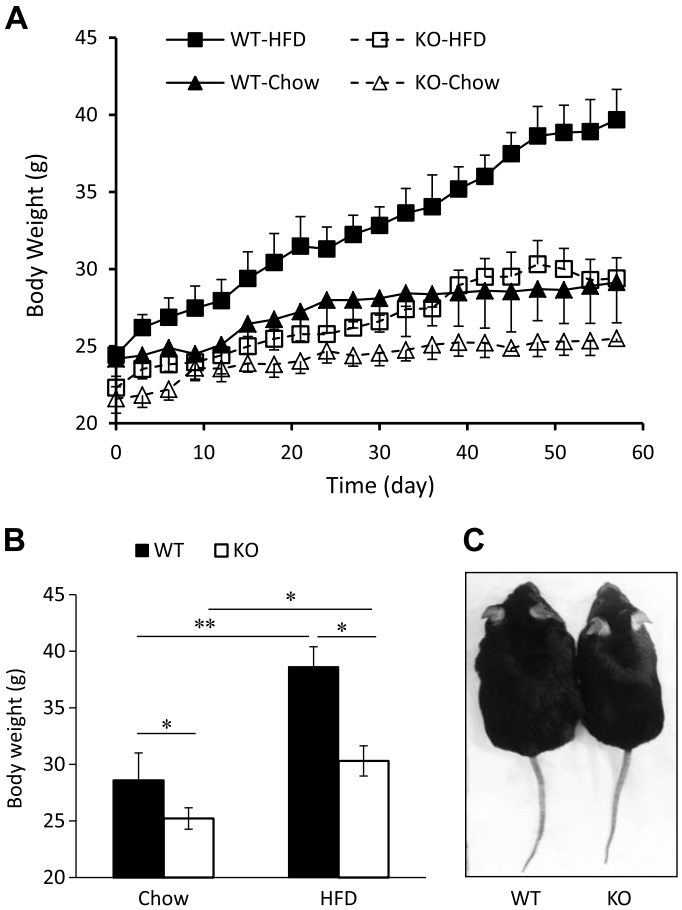

Fig. 1. Spinophilin (SPL) knockout (KO) mice are resistant to high-fat diet (HFD)-induced obesity. *A*: growth curve of male wild-type (WT) and SPL KO mice fed chow or an HFD. *B*: body weights of WT and KO mice after 8 wk of feeding of chow or an HFD. Data are presented as means ± SD; $n = 9$. *C*: male WT (*left*) and KO (*right*) mice fed an HFD for 8 wk. $^{**}P < 0.01$, $^{*}P < 0.05$, two-way ANOVA.

and total adiponectin concentrations in plasma samples were measured using enzyme-linked immunosorbent assay kits as recommended by the manufacturer (cat. no. ELM-Leptin, and EIAM-ACRP; RayBiotech, Peachtree Corners, GA).

Real-time PCR analysis. RNA was extracted from white adipose tissue. Concentration and quality of RNA according to optical density (OD) measurement. RNA was reverse transcribed into cDNA using an RT-PCR kit from Bio-Rad. SsoAdvanced Universal SYBR Green Supermix was used in a quantitative RT-PCR in a CFX96 real-time PCR detection system (Bio-Rad) to determine mRNA expression levels of UCP-1, pgc-1α, cd137, and cidea, as described previously (12). The following primer pairs were used: UCP-1: forward, 5′-AGGCTTCCAGTACCATTAGGT-3′ and reverse, 5′-CTGAGTGAGGCAAAGCTGATTT-3′; pgc-1α: forward 5′-AGCCGTGACCACTGACAACGAG-3′ and 5′-GCTGCATGGTTCTGAGTGCTAAG-3′; cd137: forward, 5′-CGTGCAGAACTCCTGTGATAAC-3′ and reverse, 5′-GTCCACCTATGCTGGAGAAGG-3′; cidea: 5′-TGCTCTTCTGTATCGCCCAGT-3′, 5′-GCCGTGTTAAGGAATCTGCTG-3′. The PCR ran for 3 min at 95°C, followed by 40 cycles with an incubation at 95°C for 15 s, 60°C for 30 s, 65°C for 10 s, and 95°C for 5 s. Relative quantification of all target genes was analyzed on the basis of a comparative cycle cross-threshold method. The amount of target genes, normalized to β-actin, were plotted and compared between groups.

Western blot analysis. Cell lysates from tissues were prepared using IP lysis buffer (Thermo Scientific, Waltham, MA). Cell lysates were resolved on 4–12% NuPAGE gels (Invitrogen, Carlsbad, CA) and transferred to PVDF membrane (Thermo Scientific). Membranes were probed with diluted antibodies (1:1,000) against Akt (Cell Signaling Technology, Danvers, MA), phospho-Ser-473 Akt (Cell Signaling), and UCP-1 (Sigma). Sheep anti-mouse (1:5,000) and goat-anti-rabbit (1:5,000) antibodies (Cell Signaling Technology) coupled to peroxidase were used to detect primary antibodies. Blots were developed with ECL advance reagent (Thermo Scientific). Protein expression levels were quantified using ImageJ software. β-actin was used as a loading control for normalization.

Hematoxylin and eosin staining. Liver or adipose tissues were fixed in 10% buffered formalin overnight, embedded in paraffin, and sectioned. Sections were rinsed with water and dehydrated in ascending alcohol solutions. Dehydrated sections were then cleared with xylene, immersed in filtered hematoxylin, and stained with eosin. Slides were finally mounted with a coverslip and observed under a light microscope. Adipose cell areas were measured using Integrated Performance Primitives image analysis software version 6.0. Four random fields were analyzed for each mouse.

Locomotor activity measurement. Locomotor activity was measured on a Versa Max Animal Activity Monitoring System (Accu Scan Instruments, Columbus, OH) using Plexiglas activity chambers

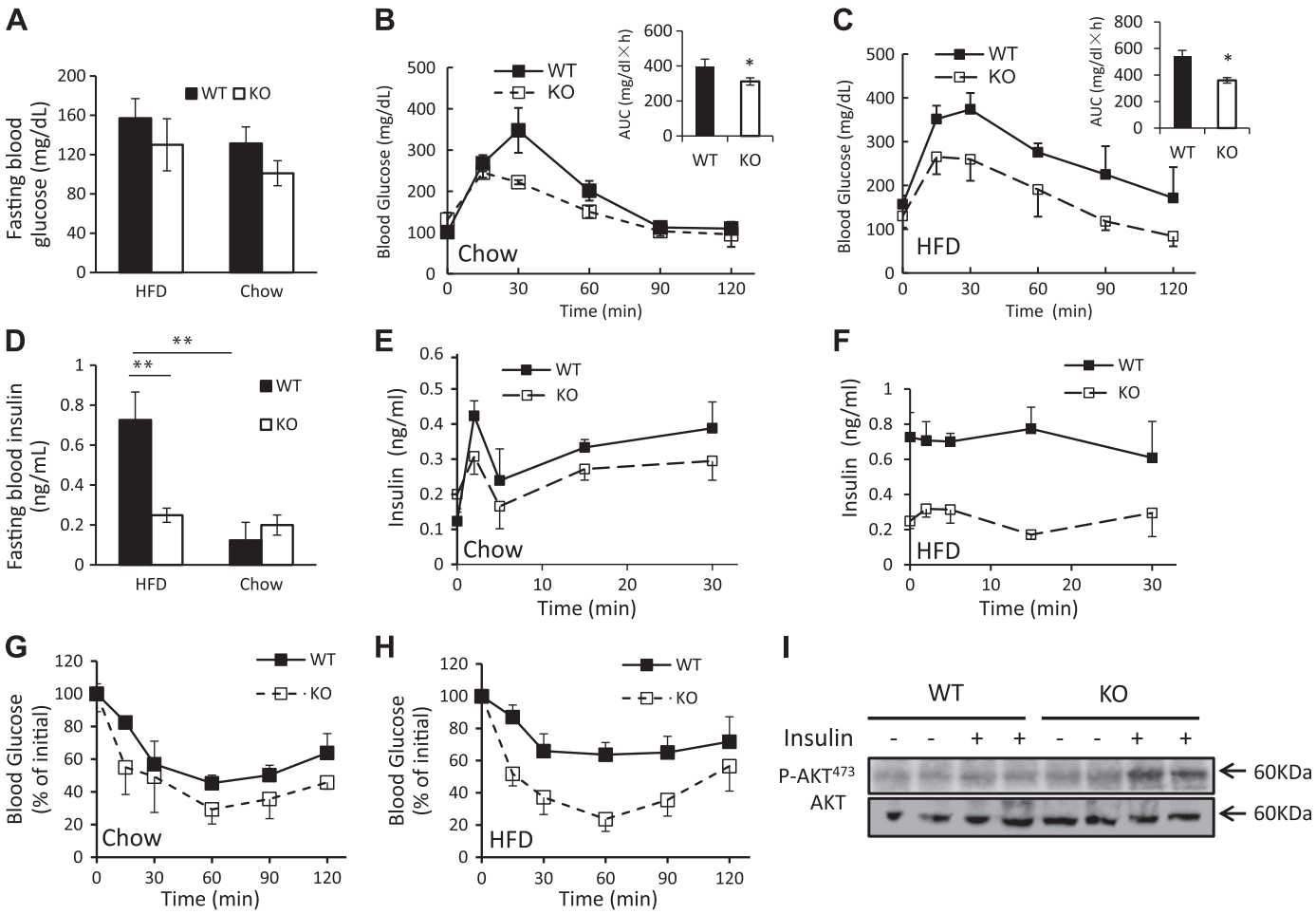

Fig. 2. Spinophilin (SPL) knockout (KO) mice are resistant to a high-fat diet (HFD)-induced hyperinsulinemia and insulin resistance. *A*: fasting blood glucose levels of wild-type (WT) and KO mice fed an HFD or chow. Intraperitoneal glucose tolerance test (IPGTT) of WT and KO mice fed chow (*B*) or an HFD (*C*). *D*: fasting plasma insulin levels of WT and KO mice fed an HFD or chow. Glucose-stimulated insulin release by WT and KO mice fed chow (*E*) or an HFD (*F*). Insulin tolerance test of WT and KO mice fed chow (*G*) or an HFD (*H*). *I*: insulin-induced phosphorylation of Akt at Ser-473 determined in liver tissues from WT and KO mice fed an HFD (n = 5–7 mice per group). $^{**}P < 0.01$, $^{*}P < 0.05$, two-way ANOVA.

(40 cm × 40 cm × 35 cm) fully covered by a black curtain. The system consisted of a Digiscan16 analyzer that monitored the state of 30 infrared beams forming a horizontal X-Y grid over the bottom of the activity chamber, and a computer interface with Versa Max software that captured consecutive horizontal beam breaks to determine total distance traveled (cm) during a 60-min test period. All experiments were carried out between 0800 and 1500 in a room with lights on.

Statistical analysis. Data are expressed as means ± SD. Differences between groups were compared for statistical significance by Student's *t* test, One-way or two-way ANOVA was performed as appropriate; $P < 0.05$ denoted significance.

RESULTS

SPL KO mice gain less weight than WT controls when fed chow or a high-fat diet. To assess the effect of SPL gene deficiency on mouse metabolism and HFD-induced obesity, 8-wk-old SPL KO and WT littermate controls were fed a control chow diet (Chow) or high-fat diet (HFD) over a period of 8 wk. Male WT mice fed Chow diet showed steady body weight gain: the body weight increased from 24.2 ± 1.1 at 8 wk to 29.1 ± 1.3 g at 16 wk (Fig. 1*A*). In contrast, the average body weights of SPL KO mice were 21.6 ± 0.9 at *week 8* and 25.5 ± 0.9 g at *week 16*. Although SPL KO mice were slightly smaller at 8 wk when the experiments were initiated, WT mice showed significantly more body weight gain than SPL KO mice. The total body weight gained during the 8-wk experiment was 4.9 ± 0.7 g in WT mice and 3.9 ± 0.7 g in SPL KO ($n = 9$ per group; $P < 0.05$, Fig. 1*A*). When fed an HFD, WT male mice became obese, with an average body weight of 38.6 ± 1.8 g ($n = 9$, Fig. 1*A*), while SPL KO mice remained lean, with an average body weight of 30.3 ± 1.3 g ($n = 9$; $P < 0.05$ vs. WT, Fig. 1, *B* and *C*). The average difference in weight gain between WT and SPL KO mice was 8.3 ± 1.9 g in SPL KO ($n = 9$ per group; $P < 0.05$, Fig. 1*B*).

Eight-week old female SPL KO mice also exhibited significantly lower body weights than WT littermate controls, and these differences persisted throughout the duration of the experiment (Supplemental Fig S1, *A* and *B*; all Supplemental material is available at https://doi.org/10.6084/m9.figshare.12567788.v1). However, weight gain among female SPL KO mice fed an HFD was similar to female WT mice fed an HFD, and no differences in body weights were seen between SPL KO and WT females over the course of the experiment (Supplemental Fig. S1, *A* and *C*), suggesting sex-based differences in body weight gain in SPL KO mice fed an HFD.

SPL KO mice are protected from high-fat diet-induced insulin resistance. As high-fat diet-induced obesity is often associated with changes in glucose metabolism, we measured fasting blood glucose levels in WT and SPL KO mice fed chow or an HFD. In male mice, no significant differences were observed in blood glucose levels between WT and SPL KO fed either chow or an HFD (Fig. 2*A*). When mice were challenged with high glucose during an IPGTT test (2 mg/g of D-glucose), SPL KO mice fed either diet exhibited lower serum glucose levels than WT mice at most time points, as well as reduced areas under the curve (Fig. 2, *B* and C, *insets*), indicating more efficient glucose metabolism in SPL KO mice. WT and SPL KO mice fed chow had similar fasting serum insulin levels. However, in mice fed an HFD, elevated serum insulin was observed in WT but not in SPL KO mice (Fig. 2*D*).

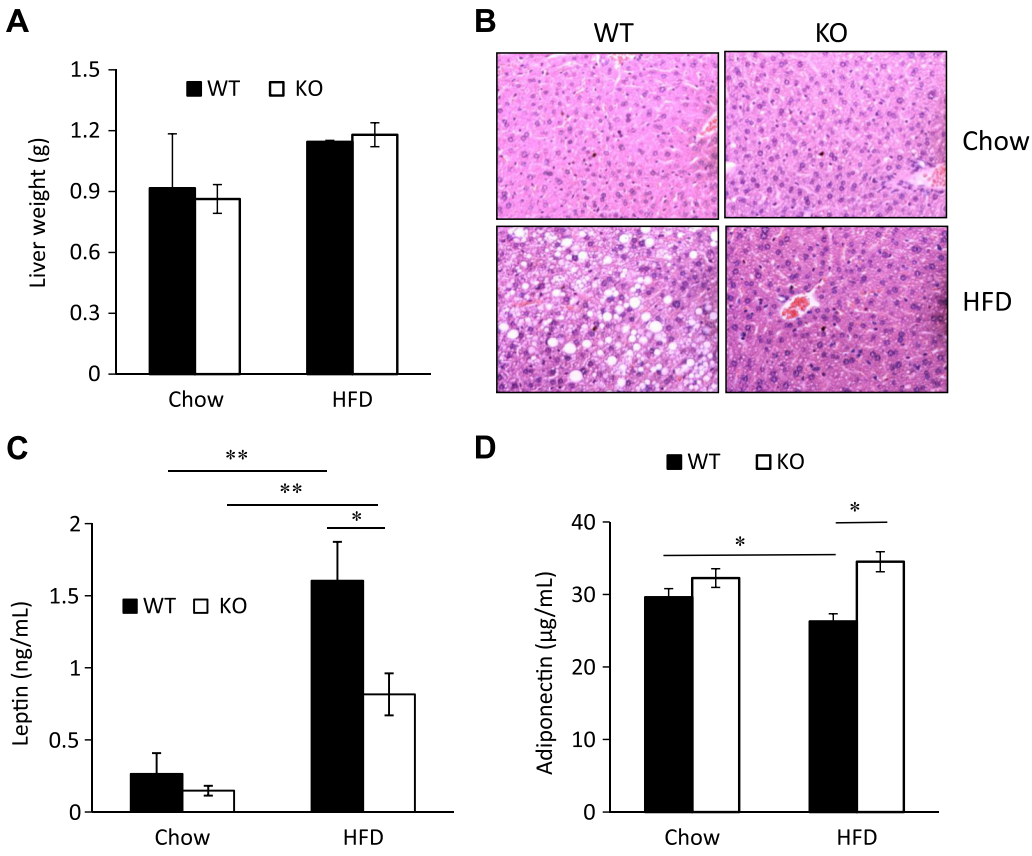

Fig. 3. Liver steatosis and adipokine secretion in spinophilin (SPL) knockout (KO) and control mice. *A*: liver weights of chow-fed and high-fat diet (HFD)-fed wild-type (WT) and KO mice. *B*: hematoxylin-and-eosin-stained sections of liver tissues from chow-fed and HFD-fed WT and KO mice. Serum leptin (*C*) and adiponectin (*D*) levels of chow-fed and HFD-fed WT and KO mice (n = at least four mice per group). $^{**}P < 0.01$, $^{*}P < 0.05$, two-way ANOVA.

Table 1. *Average food and caloric intake in male WT and SPL KO mice per 24 h*

	Chow		HFD	
	WT	KO	WT	KO
Food intake per day, g	3.0 ± 0.2	3.4 ± 0.2*	2.5 ± 0.2	2.8 ± 0.2**
Caloric intake per day, kcal	11.5 ± 0.7	13.1 ± 0.7	13.1 ± 1.0	14.7 ± 1.0

Values are expressed as means ± SE. $n = 9$ in each group. Food intake was measured twice a week over an 8-wk period of dietary intervention. HFD, high-fat diet; KO, knockout; SPL, spinophilin; WT, wild-type. $^{**}P < 0.01$, $^{*}P < 0.05$ vs. corresponding WT.

We next measured insulin release stimulated by injection of glucose (3 mg/g ip). SPL KO mice fed chow secreted less insulin than their WT littermates, but the difference did not reach significance (Fig. 2*E*). In contrast, in mice fed an HFD, insulin secretion was much lower in SPL KO than WT mice (Fig. 2*F*), suggesting that depletion of the SPL gene inhibits insulinemia induced by a high-fat diet. Nevertheless, we do not exclude the possibility that reduced insulin secretion could result from better insulin sensitivity in KO mice that required less insulin to maintain euglycemia.

Next, we measured insulin sensitivity in male mice by ITT. SPL KO mice fed chow or an HFD exhibited greater insulin sensitivity than the corresponding WT controls (Fig. 2, *G* and *H*), suggesting that the absence of SPL protects male SPL KO mice from an HFD-induced insulin resistance. As a possible mechanism, we examined the activities of the insulin-signaling intermediate Akt. We observed that phosphorylation of Akt was increased in livers of insulin-treated HFD-fed SPL KO mice (Fig. 2*I*), suggesting that deletion of SPL increases insulin sensitivity via promoting insulin signaling.

GTT and ITT were also performed in female mice after 8 wk of chow or HFD feeding. Female KO mice fed chow diet show better glucose disposal than WT mice (Supplemental Fig. S2*A*, *inset*). However, no differences in glucose disposal or insulin sensitivity were observed between WT and SPL KO female mice fed an HFD diet (Supplemental Fig. S2, *A–D*).

SPL KO mice were protected from an HFD-induced hepatic steatosis and showed reduced leptin levels and elevated adiponectin levels. A high-fat diet is known to induce liver steatosis. Therefore, we measured the effects of SPL ablation on liver weight and steatosis. We found no difference in liver weights between male SPL KO and WT mice fed either chow or an HFD (Fig. 3*A*). However, hepatic steatosis was prominent in WT livers but was not observed in SPL KO livers (Fig. 3*B*), indicating that SPL deficiency protects against HFD-induced hepatic steatosis. Adipokines produced by WAT, including leptin and adiponectin, play critical roles in regulating insulin sensitivity and energy balance. We measured serum leptin and adiponectin levels in WT and SPL KO male mice fed chow or an HFD. There was no difference in leptin and adiponectin levels among SPL KO and WT mice fed chow (Fig. 3, *C* and *D*). In contrast, SPL KO mice fed an HFD showed significantly lower leptin levels and elevated adiponectin levels compared with WT mice fed an HFD (Fig. 3,

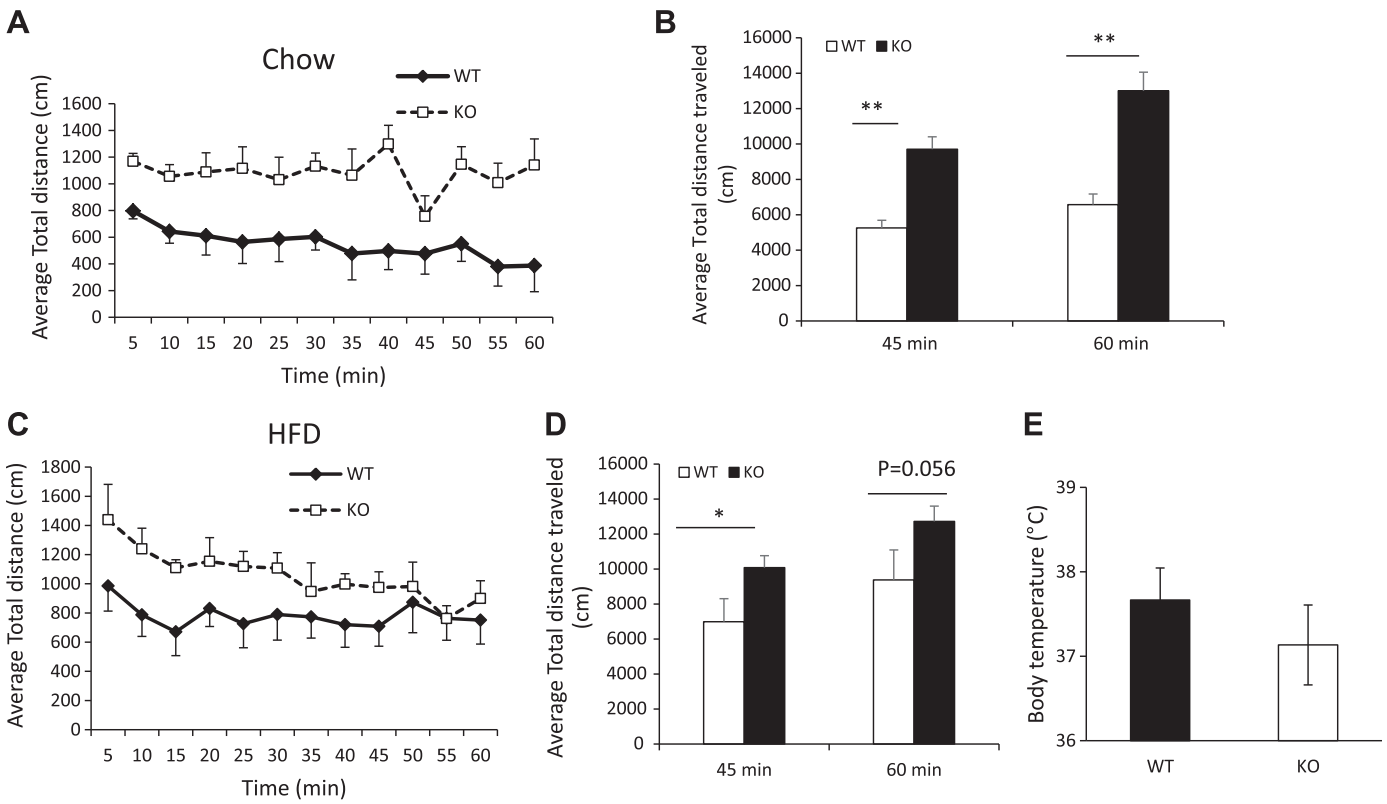

Fig. 4. Locomotor activity of male wild-type (WT) and knockout (KO) mice. *A*: average distance traveled in 5-min intervals by chow-fed WT and spinophilin (SPL) KO mice. *B*: total distance traveled within 60 min in chow-fed WT and SPL KO mice. *C*: distance traveled in 5-min intervals by HFD-fed WT and SPL KO mice. *D*: total distance traveled within 60 min by HFD-fed WT and SPL KO mice. *E*: body temperature of chow-fed WT and SPL KO mice. Result shown is representative of at least three independent experiments ($n = 6–8$ per group for each experiment). $^{**}P < 0.01$, $^{*}P < 0.05$, Student's *t* test.

C and *D*), suggesting that one of the mechanisms by which deletion of SPL restores insulin sensitivity is by reversing the alteration of adipokine levels caused by an HFD.

Food intake and physical activity in SPL KO and control mice. Resistance to an HFD-induced obesity is often due to lower food intake and/or higher energy expenditure. However, analysis of food intake and caloric intake in our study showed that SPL KO mice fed either chow or an HFD ate somewhat more than corresponding controls (Table 1), suggesting that reduced obesity of male SPL KO mice was not a consequence of reduced food intake. We postulated that SPL KO mice expended more energy than WT mice through increased physical activity. Physical activity of mice was measured using the Animal Activity Monitoring System. We found that the average total distance traveled was 10,040 ± 2,117 cm in Chow-SPL KO and 5,879 ± 1,048 cm in chow WT mice during the first 45 min of the locomotor session, and 12,002 ± 2,578 cm (KO) vs. 6,575 ± 1,584 cm (WT) for the complete 60-min locomotor session (Fig. 4, *A* and *B*). After feeding the HFD, SPL KO mice had greater distance traveled compared with WT mice in the first 45 min of the session (SPL KO: 10,086 ± 680 cm; WT: 6,991 ± 1,315 cm; $P = 0.03$), with an average total distance traveled during the entire test period of 12,728 ± 2,134 cm in HFD-fed SPL KO vs. 9,378 ± 4,205 cm in HFD-fed WT mice ($P = 0.056$; Fig. 4, *C* and *D*).

Chow-fed female SPL KO mice also exhibited increased locomotor activity compared with WT controls (Supplemental Fig. S3, *A* and *B*). However, no differences were observed in HFD-fed SPL KO and WT female mice (Supplemental Fig. S3, *C* and *D*). In addition, there were no significant differences in body temperatures between chow- or HFD-fed mice of either sex (Fig. 4*E* and Supplemental Fig. S3*E*).

Ablation of SPL reduces iWAT and vWAT tissue weights. We hypothesized that differences in body weights between SPL KO and WT male mice were caused by the reduction of adipose tissue deposits. In both chow-fed and HFD-fed mice, we found that SPL KO mice had significantly reduced BAT, vWAT, and inguinal white adipose tissue (iWAT) compared with WT controls (Fig. 5, *A*–*C*). Using hematoxylin-and-eosin staining, we also found that adipocytes in vWAT from both Chow- and HFD-fed SPL KO mice were smaller than in WT controls (Fig. 5, *D* and *E*).

Enhanced expression of markers of browning in SPL KO mice. To determine the effects of SPL depletion on expression of browning-related genes in WAT, we measured mRNA expression of UCP-1, pgc-1α, cd137, and cidea in iWAT and

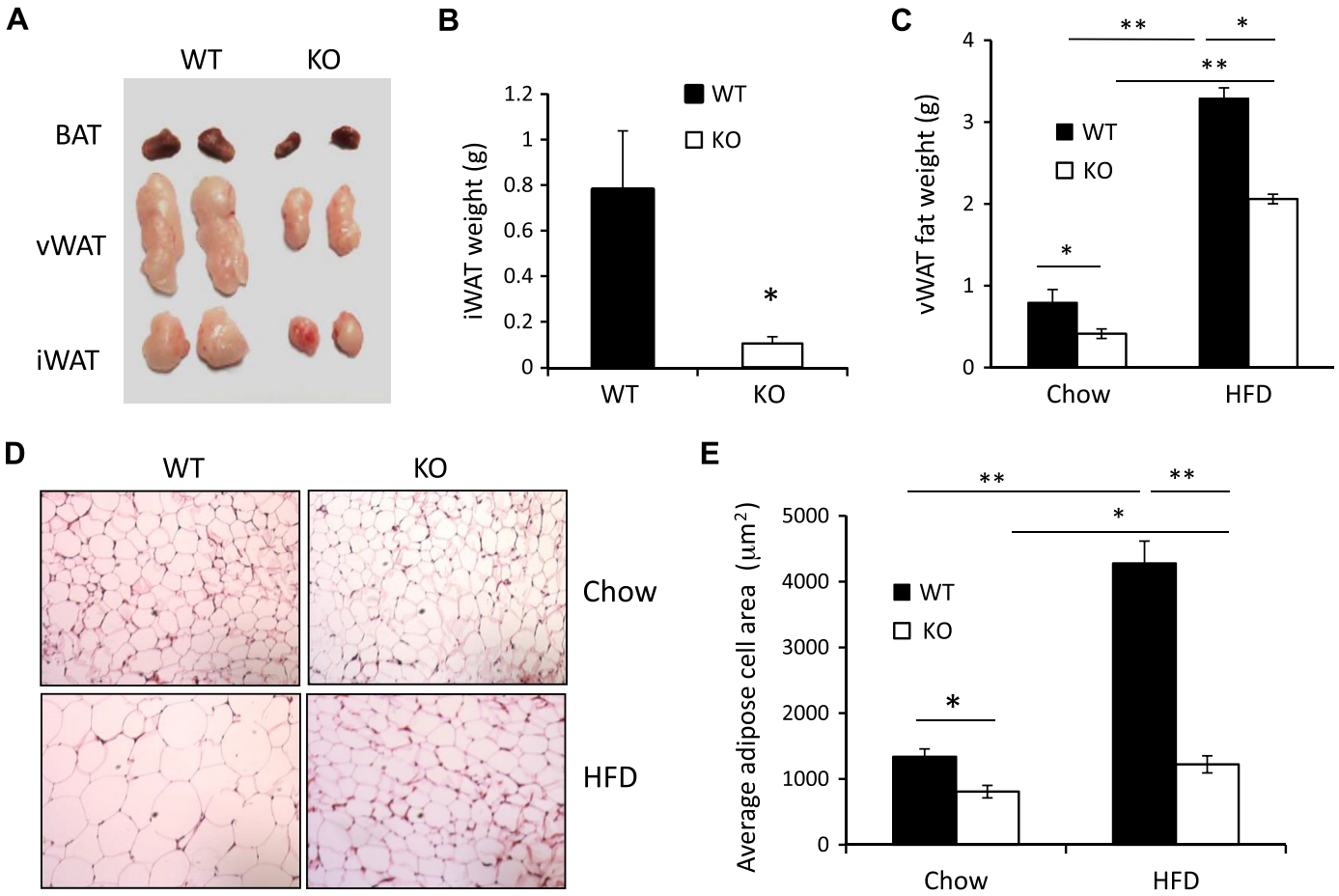

Fig. 5. Depletion of spinophilin (SPL) reduces obesity. *A*: representative images of brown adipose tissue (BAT), visceral white adipose tissue (vWAT), and inguinal white adipose tissue (iWAT) from male wild-type (WT) and knockout (KO) mice. *B*: iWAT weights of chow-fed and high-fat diet (HFD)-fed (KO) and WT mice. *C*: vWAT weights of chow-fed KO and WT mice. *D*: hematoxylin-and-eosin-stained sections of vWAT from chow-fed and HFD-fed WT and KO mice. *E*: adipose cell areas were measured using Integrated Performance Primitives image analysis software version 6.0. Four random fields were analyzed for each mouse. $n = 5$. $^{**}P < 0.01$, $^{*}P < 0.05$, two-way ANOVA.

vWAT from male SPL KO and WT control mice fed a chow diet. There were no significant differences between SPL KO and WT mice in expression of these genes in iWAT (Fig. 6*A*). However, expression of UCP-1 was significantly increased in vWAT from SPL KO mice compared with WT controls (Fig. 6*B*). In addition, we have observed increased expression of cd137 and cidea (Fig. 6*B*), two markers for mitochondrial activity. Increased UCP-1 gene expression was further demonstrated in vWAT tissue sections from SPL KO mice by immunofluorescent staining (Fig. 6*C*) and Western blot analysis (Fig. 6, *D* and *E*). These data indicate that browning happened in vWAT of SPL KO mice, and the browning effect of SPL ablation depends on the location of WAT.

DISCUSSION

This study sheds light on the mechanism of SPL action in obesity. We found that SPL KO mice had better glucose homeostasis and were resistant to HFD-induced obesity and insulin resistance compared with their WT littermates, which was, at least in part, due to increased physical activity and browning of white adipocytes in the vWAT depot. High-fat diet induces obesity, which is associated with type 2 diabetes mellitus and related metabolic disturbances, including hyperglycemia, hyperinsulinemia, insulin resistance, and hepatosteatosis. Identification of genes contributes to obesity, and its complication can help develop drug targets for therapy. Our data showed that SPL gene expression was required for the development of obesity and insulin resistance in C57BL/6 mice. SPL KO mice fed normal chow were leaner and had increased insulin sensitivity compared with age-matched, wild-type littermates. After 8 wk of high-fat-diet feeding, SPL KO mice exhibited markedly reduced weight gain, reduced body fat, and enhanced physical activity compared with WT littermate controls. They also exhibited better glucose tolerance and insulin sensitivity. We found increased expression of the brown adipose tissue marker (UCP-1) and increased expression

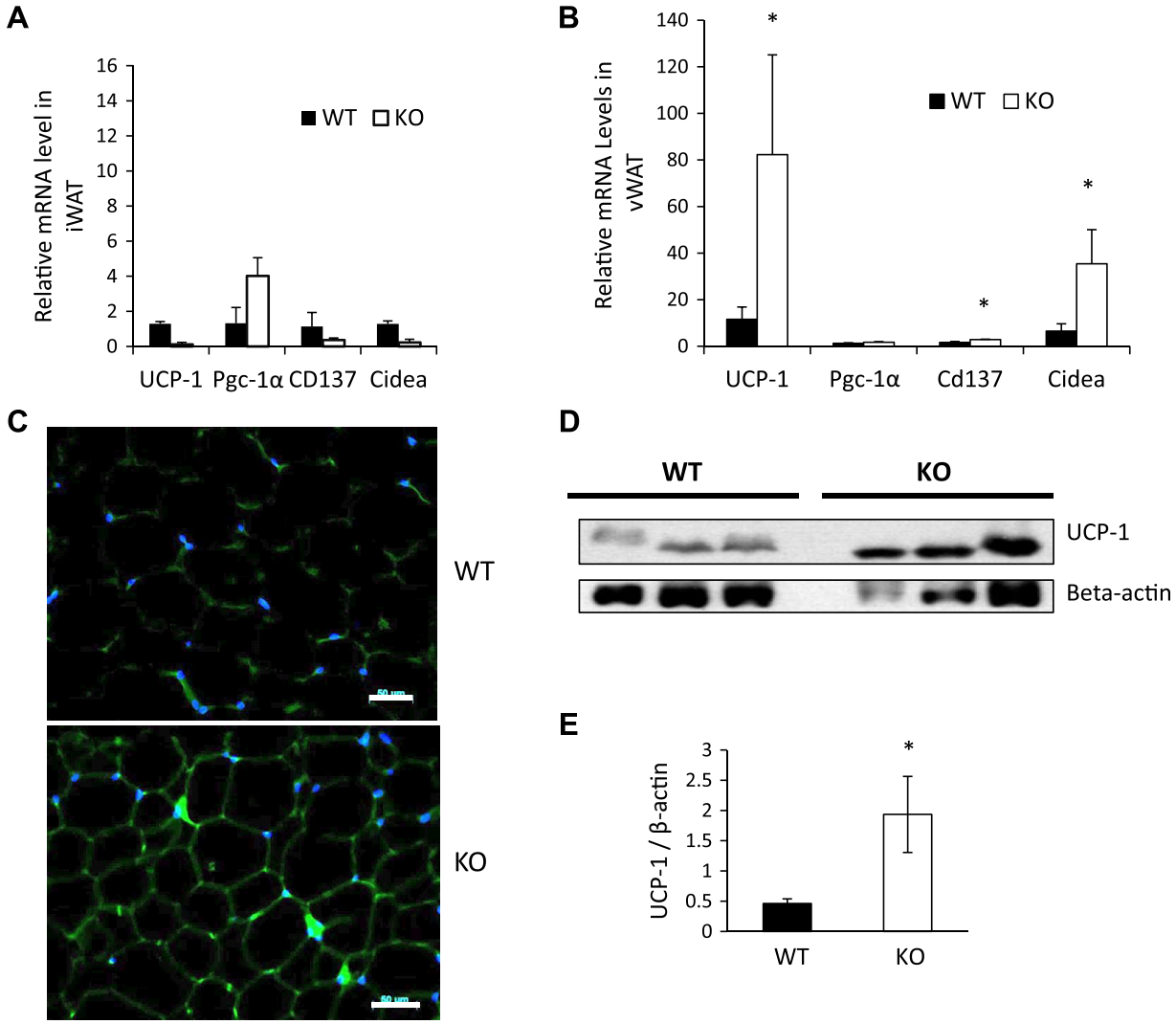

Fig. 6. Increased uncoupling protein-1 (UCP-1) and cidea expression in visceral white adipose tissue (vWAT) from male spinophilin (SPL) knockout (KO) mice. Relative mRNA levels of genes related to browning in inguinal white adipose tissue (iWAT) (*A*) and vWAT (*B*) harvested from wild-type (WT) or SPL KO mice. *C*: immunofluorescence staining of UCP1 in vWAT of WT and SPL KO mice. *D*: Western blot analysis of UCP-1 gene expression in WT and SPL KO mice (β-actin was used as a normalization control). *E*: quantification of UCP-1 protein expression using ImageJ software (*G*). *$P < 0.05$ vs. corresponding WT, using Student's *t* test.

of markers of mitochondrial activity and function (CD137 and cidea) in visceral white adipose tissue from SPL KO mice, suggesting that ablation of SPL improves glucose homeostasis at least in part by promoting browning of white adipocytes.

There are two major WAT depots in rodents and humans: visceral (vWAT) and subcutaneous (scWAT). vWAT and scWAT are differentially associated with health risks. For example, vWAT is associated with insulin resistance, increased risk of T2D, atherosclerosis, and mortality (3–5), whereas, scWAT is associated with increased insulin sensitivity and reduction in T2D (6, 7). Glucose homeostasis is regulated by a number of different factors that promote browning of different WAT depots. For example, reduction of Receptor Interacting Protein 140 expression facilitates browning in vWAT (21); LGR4 ablation potentiates browning in vWAT (39), and exercise training causes beiging in scWAT (5, 38). Here, we found that ablation of SPL selectively induced browning of vWAT.

Physical activity and exercise are positively correlated with energy expenditure and can increase whole-body glucose utilization and decrease blood glucose levels in patients with T2D (35, 36). We observed increased locomotor activity in SPL KO mice. It has been shown that SPL KO mice exhibit a deficiency in long-term depression, which may lead to increased activity (2, 6, 15). On the basis of our data, we postulate that enhanced locomotor activity promotes browning of vWAT in SPL KO mice. Indeed, we observed that the effect of SPL ablation on WAT browning shares many similarities with exercise-induced browning. For example, both improve whole body glucose homeostasis and energy expenditure. Both lead to decreased circulating leptin and increased adiponectin levels, which play important roles in the regulation of whole body glucose homeostasis (17, 42). Unlike cold exposure or pharmaceutical agents that cause beiging through increased heat loss and possible compensatory adrenergic stimulation, exercise or SPL KO ablation does not increase heat loss or heat production (19, 25), i.e., the body temperatures of SPL KO mice were similar to controls. Nevertheless, activity-independent mechanisms also appeared to contribute to the browning of vWAT in SPL KO mice. Physical activity and exercise lead primarily to browning in scWAT rather than vWAT; whereas, we observed browning in vWAT in SPL KO mice. Of note, in SPL KO mice, expression of markers of mitochondrial activity, cidea and cd137, were increased in vWAT compared with WT controls, whereas, genes related to exercise-induced browning including Pgc-1α, a marker for mitochondrial biogenesis (37), were not affected by SPL ablation, suggesting that SPL plays a role in regulating mitochondrial activity rather than mitochondrial biogenesis in vWAT of SPL KO mice.

Our data do not explain why depletion of the SPL gene resulted in different phenotypes in male and female mice. While we suspect that hormonal differences may be the cause, further studies will be needed to answer this question. In addition, because the SPL KO mice used in this study were whole genome knockout, we cannot exclude the possibility that other factors contribute to the different metabolic phenotypes observed in this study. These issues may be resolved by analysis of tissue-specific knockout mice.

While not a focus of this study, but of interest for future studies, is whether the phenotype observed in the SPL KO mice was from the reduction of body weight gain or directly from insulin sensitivity, or both. In addition, dyslipidemia and blood pressure elevation are often observed in HFD-fed mice in addition to insulin resistance, which will be evaluated in future studies.

In conclusion, we found that SPL gene expression was required for the development of obesity and insulin resistance in C57BL/6 mice. Furthermore, expression of UCP-1 and other markers of mitochondrial activity and function in visceral white adipose tissue from SPL KO mice, suggesting that ablation of SPL improves glucose homeostasis, at least in part by promoting browning of white adipocytes. Our data suggest that SPL may be a novel target to reduce obesity and its related complications in patients.

GRANTS

This study was supported by the National Institute of Health National Institute of Diabetes and Digestive and Kidney Diseases Grants 1R01DK-105183, DK-120394, DK-118529, and the Department of Veterans Affairs (VA Office of Research & Development, Biomedical Laboratory Research and Development Merit I01BX004536) to H.W.

DISCLOSURES

No conflicts of interest, financial or otherwise, are declared by the authors.

AUTHOR CONTRIBUTIONS

Y.Z. and H.W. conceived and designed research; Y.Z., L.S., H.D., D.-s.K., and Z.S. performed experiments; Y.Z., L.S., and Z.S. analyzed data; Y.Z., L.S., and Q.W. interpreted results of experiments; Y.Z. and L.S. prepared figures; Y.Z., H.B., and H.W. drafted manuscript; Y.Z., L.S., H.D., D.-s.K., Z.S., H.B., Q.W., and H.W. approved final version of manuscript.

REFERENCES

1. **Allen PB, Ouimet CC, Greengard P.** Spinophilin, a novel protein phosphatase 1 binding protein localized to dendritic spines. *Proc Natl Acad Sci USA* 94: 9956–9961, 1997. doi:10.1073/pnas.94.18.9956.
2. **Allen PB, Zachariou V, Svenningsson P, Lepore AC, Centonze D, Costa C, Rossi S, Bender G, Chen G, Feng J, Snyder GL, Bernardi G, Nestler EJ, Yan Z, Calabresi P, Greengard P.** Distinct roles for spinophilin and neurabin in dopamine-mediated plasticity. *Neuroscience* 140: 897–911, 2006. doi:10.1016/j.neuroscience.2006.02.067.
3. **Bloom O, Unternaehrer JJ, Jiang A, Shin JS, Delamarre L, Allen P, Mellman I.** Spinophilin participates in information transfer at immunological synapses. *J Cell Biol* 181: 203–211, 2008. doi:10.1083/jcb.200711149.
4. **Bonet ML, Oliver P, Palou A.** Pharmacological and nutritional agents promoting browning of white adipose tissue. *Biochim Biophys Acta* 1831: 969–985, 2013. doi:10.1016/j.bbalip.2012.12.002.
5. **Boström P, Wu J, Jedrychowski MP, Korde A, Ye L, Lo JC, Rasbach KA, Boström EA, Choi JH, Long JZ, Kajimura S, Zingaretti MC, Vind BF, Tu H, Cinti S, Højlund K, Gygi SP, Spiegelman BM.** A PGC1-α-dependent myokine that drives brown-fat-like development of white fat and thermogenesis. *Nature* 481: 463–468, 2012. doi:10.1038/nature10777.
6. **Buyukdura JS, McClintock SM, Croarkin PE.** Psychomotor retardation in depression: biological underpinnings, measurement, and treatment. *Prog Neuropsychopharmacol Biol Psychiatry* 35: 395–409, 2011. doi:10.1016/j.pnpbp.2010.10.019.
7. **Cao L, Choi EY, Liu X, Martin A, Wang C, Xu X, During MJ.** White to brown fat phenotypic switch induced by genetic and environmental activation of a hypothalamic-adipocyte axis. *Cell Metab* 14: 324–338, 2011. doi:10.1016/j.cmet.2011.06.020.
8. **Charlton JJ, Allen PB, Psifogeorgou K, Chakravarty S, Gomes I, Neve RL, Devi LA, Greengard P, Nestler EJ, Zachariou V.** Multiple actions of spinophilin regulate μ opioid receptor function. *Neuron* 58: 238–247, 2008. doi:10.1016/j.neuron.2008.02.006.
9. **Cottingham C, Li X, Wang Q.** Noradrenergic antidepressant responses to desipramine in vivo are reciprocally regulated by arrestin3 and spinophilin. *Neuropharmacology* 62: 2354–2362, 2012. doi:10.1016/j.neuropharm.2012.02.011.

10. **Cousin B, Cinti S, Morroni M, Raimbault S, Ricquier D, Pénicaud L, Casteilla L.** Occurrence of brown adipocytes in rat white adipose tissue: molecular and morphological characterization. *J Cell Sci* 103: 931–942, 1992.
11. **da Costa-Goncalves AC, Tank J, Plehm R, Diedrich A, Todiras M, Gollasch M, Heuser A, Wellner M, Bader M, Jordan J, Luft FC, Gross V.** Role of the multidomain protein spinophilin in blood pressure and cardiac function regulation. *Hypertension* 52: 702–707, 2008. doi:10.1161/HYPERTENSIONAHA.108.114355.
12. **Dong H, Huang H, Yun X, Kim DS, Yue Y, Wu H, Sutter A, Chavin KD, Otterbein LE, Adams DB, Kim YB, Wang H.** Bilirubin increases insulin sensitivity in leptin-receptor deficient and diet-induced obese mice through suppression of ER stress and chronic inflammation. *Endocrinology* 155: 818–828, 2014. doi:10.1210/en.2013-1667.
13. **Enerbäck S.** Human brown adipose tissue. *Cell Metab* 11: 248–252, 2010. doi:10.1016/j.cmet.2010.03.008.
14. **Fabbrini E, Sullivan S, Klein S.** Obesity and nonalcoholic fatty liver disease: biochemical, metabolic, and clinical implications. *Hepatology* 51: 679–689, 2010. doi:10.1002/hep.23280.
15. **Feng J, Yan Z, Ferreira A, Tomizawa K, Liauw JA, Zhuo M, Allen PB, Ouimet CC, Greengard P.** Spinophilin regulates the formation and function of dendritic spines. *Proc Natl Acad Sci USA* 97: 9287–9292, 2000. doi:10.1073/pnas.97.16.9287.
16. **Ferrer I, Blanco-Aparicio C, Peregrina S, Cañamero M, Fominaya J, Cecilia Y, Lleonart M, Hernandez-Losa J, Ramon y Cajal S, Carnero A.** Spinophilin acts as a tumor suppressor by regulating Rb phosphorylation. *Cell Cycle* 10: 2751–2762, 2011. doi:10.4161/cc.10.16.16422.
17. **Golbidi S, Laher I.** Exercise induced adipokine changes and the metabolic syndrome. *J Diabetes Res* 2014: 726861, 2014. doi:10.1155/2014/726861.
18. **Gollisch KS, Brandauer J, Jessen N, Toyoda T, Nayer A, Hirshman MF, Goodyear LJ.** Effects of exercise training on subcutaneous and visceral adipose tissue in normal- and high-fat diet-fed rats. *Am J Physiol Endocrinol Metab* 297: E495–E504, 2009. doi:10.1152/ajpendo.90424.2008.
19. **Hirata M, Suzuki M, Ishii R, Satow R, Uchida T, Kitazumi T, Sasaki T, Kitamura T, Yamaguchi H, Nakamura Y, Fukami K.** Genetic defect in phospholipase Cδ1 protects mice from obesity by regulating thermogenesis and adipogenesis. *Diabetes* 60: 1926–1937, 2011. doi:10.2337/db10-1500.
20. **James WP.** The epidemiology of obesity: the size of the problem. *J Intern Med* 263: 336–352, 2008. doi:10.1111/j.1365-2796.2008.01922.x.
21. **Liu PS, Lin YW, Lee B, McCrady-Spitzer SK, Levine JA, Wei LN.** Reducing RIP140 expression in macrophage alters ATM infiltration, facilitates white adipose tissue browning, and prevents high-fat diet-induced insulin resistance. *Diabetes* 63: 4021–4031, 2014. doi:10.2337/db14-0619.
22. **Lu R, Chen Y, Cottingham C, Peng N, Jiao K, Limbird LE, Wyss JM, Wang Q.** Enhanced hypotensive, bradycardic, and hypnotic responses to alpha2-adrenergic agonists in spinophilin-null mice are accompanied by increased G protein coupling to the alpha2A-adrenergic receptor. *Mol Pharmacol* 78: 279–286, 2010. doi:10.1124/mol.110.065300.
23. **Murphy NF, MacIntyre K, Stewart S, Hart CL, Hole D, McMurray JJ.** Long-term cardiovascular consequences of obesity: 20-year follow-up of more than 15,000 middle-aged men and women (the Renfrew-Paisley study). *Eur Heart J* 27: 96–106, 2006. doi:10.1093/eurheartj/ehi506.
24. **Nedergaard J, Bengtsson T, Cannon B.** Unexpected evidence for active brown adipose tissue in adult humans. *Am J Physiol Endocrinol Metab* 293: E444–E452, 2007. doi:10.1152/ajpendo.00691.2006.
25. **Nedergaard J, Cannon B.** The browning of white adipose tissue: some burning issues. *Cell Metab* 20: 396–407, 2014. doi:10.1016/j.cmet.2014.07.005.
26. **Nicholls DG, Locke RM.** Thermogenic mechanisms in brown fat. *Physiol Rev* 64: 1–64, 1984. doi:10.1152/physrev.1984.64.1.1.
27. **Ogden CL, Carroll MD, Flegal KM.** Prevalence of obesity in the United States. *JAMA* 312: 189–190, 2014. doi:10.1001/jama.2014.6228.
28. **V RP, Vemisetty H, K D, Reddy SJ, D R, Krishna MJ, Malathi G.** Comparative evaluation of marginal adaptation of biodentine(TM) and other commonly used root end filling materials-an in vitro study. *J Clin Diagn Res* 8: 243–245, 2014. doi:10.7860/jcdr/2014/7834.4174.
29. **Petrovic N, Walden TB, Shabalina IG, Timmons JA, Cannon B, Nedergaard J.** Chronic peroxisome proliferator-activated receptor gamma (PPARγ) activation of epididymally derived white adipocyte cultures reveals a population of thermogenically competent, UCP1-containing adipocytes molecularly distinct from classic brown adipocytes. *J Biol Chem* 285: 7153–7164, 2010. doi:10.1074/jbc.M109.053942.
30. **Rosen ED, Spiegelman BM.** Adipocytes as regulators of energy balance and glucose homeostasis. *Nature* 444: 847–853, 2006. doi:10.1038/nature05483.
31. **Ruiz de Azua I, Nakajima K, Rossi M, Cui Y, Jou W, Gavrilova O, Wess J.** Spinophilin as a novel regulator of M3 muscarinic receptor-mediated insulin release in vitro and in vivo. *FASEB J* 26: 4275–4286, 2012. doi:10.1096/fj.12-204644.
32. **Sarrouilhe D, di Tommaso A, Métayé T, Ladeveze V.** Spinophilin: from partners to functions. *Biochimie* 88: 1099–1113, 2006. doi:10.1016/j.biochi.2006.04.010.
33. **Satoh A, Nakanishi H, Obaishi H, Wada M, Takahashi K, Satoh K, Hirao K, Nishioka H, Hata Y, Mizoguchi A, Takai Y.** Neurabin-II/spinophilin. An actin filament-binding protein with one pdz domain localized at cadherin-based cell-cell adhesion sites. *J Biol Chem* 273: 3470–3475, 1998. doi:10.1074/jbc.273.6.3470.
34. **Smyth S, Heron A.** Diabetes and obesity: the twin epidemics. *Nat Med* 12: 75–80, 2006. doi:10.1038/nm0106-75.
35. **Stanford KI, Middelbeek RJ, Goodyear LJ.** Exercise effects on white adipose tissue: beiging and metabolic adaptations. *Diabetes* 64: 2361–2368, 2015. doi:10.2337/db15-0227.
36. **Stanford KI, Middelbeek RJ, Townsend KL, Lee MY, Takahashi H, So K, Hitchcox KM, Markan KR, Hellbach K, Hirshman MF, Tseng YH, Goodyear LJ.** A novel role for subcutaneous adipose tissue in exercise-induced improvements in glucose homeostasis. *Diabetes* 64: 2002–2014, 2015. doi:10.2337/db14-0704.
37. **Sutherland LN, Bomhof MR, Capozzi LC, Basaraba SA, Wright DC.** Exercise and adrenaline increase PGC-1alpha mRNA expression in rat adipose tissue. *J Physiol* 587: 1607–1617, 2009. doi:10.1113/jphysiol.2008.165464.
38. **Trevellin E, Scorzeto M, Olivieri M, Granzotto M, Valerio A, Tedesco L, Fabris R, Serra R, Quarta M, Reggiani C, Nisoli E, Vettor R.** Exercise training induces mitochondrial biogenesis and glucose uptake in subcutaneous adipose tissue through eNOS-dependent mechanisms. *Diabetes* 63: 2800–2811, 2014. doi:10.2337/db13-1234.
39. **Wang J, Liu R, Wang F, Hong J, Li X, Chen M, Ke Y, Zhang X, Ma Q, Wang R, Shi J, Cui B, Gu W, Zhang Y, Zhang Z, Wang W, Xia X, Liu M, Ning G.** Ablation of LGR4 promotes energy expenditure by driving white-to-brown fat switch. *Nat Cell Biol* 15: 1455–1463, 2013. doi:10.1038/ncb2867.
40. **Wang Q, Zhao J, Brady AE, Feng J, Allen PB, Lefkowitz RJ, Greengard P, Limbird LE.** Spinophilin blocks arrestin actions in vitro and in vivo at G protein-coupled receptors. *Science* 304: 1940–1944, 2004. doi:10.1126/science.1098274.
41. **Wu J, Cohen P, Spiegelman BM.** Adaptive thermogenesis in adipocytes: is beige the new brown? *Genes Dev* 27: 234–250, 2013. doi:10.1101/gad.211649.112.
42. **Zachwieja JJ, Hendry SL, Smith SR, Harris RB.** Voluntary wheel running decreases adipose tissue mass and expression of leptin mRNA in Osborne-Mendel rats. *Diabetes* 46: 1159–1166, 1997. doi:10.2337/diab.46.7.1159.